c-Myc Antagonises the Transcriptional Activity of the Androgen Receptor in Prostate Cancer Affecting Key Gene Networks

Published in:
EBioMedicine

Document Version:
Publisher's PDF, also known as Version of record

Queen's University Belfast - Research Portal:
Link to publication record in Queen's University Belfast Research Portal

Research Paper

c-Myc Antagonises the Transcriptional Activity of the Androgen Receptor in Prostate Cancer Affecting Key Gene Networks

CrossMark

Stefan J. Barfeld [a],[***],[1], Alfonso Urbanucci [a,b],[**],[1], Harri M. Itkonen [a], Ladan Fazli [c], Jessica L. Hicks [d], Bernd Thiede [d], Paul S. Rennie [c], Srinivasan Yegnasubramanian [e], Angelo M. DeMarzo [e], Ian G. Mills [a,b,f],[*]

[a] Centre for Molecular Medicine Norway (NCMM), Nordic EMBL Partnership, University of Oslo, Oslo, Norway
[b] Department of Molecular Oncology, Institute for Cancer Research, Oslo University Hospital, Oslo, Norway
[c] The Vancouver Prostate Centre, University of British Columbia, Canada
[d] Department of Biosciences, University of Oslo, Oslo, Norway
[e] Sidney Kimmel Comprehensive Cancer Center, Johns Hopkins School of Medicine, Baltimore, MD, USA.
[f] PCUK/Movember Centre of Excellence, CCRCB, Queen's University, Belfast, UK

ARTICLE INFO

ABSTRACT

Prostate cancer (PCa) is the most common non-cutaneous cancer in men. The androgen receptor (AR), a ligand-activated transcription factor, constitutes the main drug target for advanced cases of the disease. However, a variety of other transcription factors and signaling networks have been shown to be altered in patients and to influence AR activity. Amongst these, the oncogenic transcription factor c-Myc has been studied extensively in multiple malignancies and elevated protein levels of c-Myc are commonly observed in PCa. Its impact on AR activity, however, remains elusive. In this study, we assessed the impact of c-Myc overexpression on AR activity and transcriptional output in a PCa cell line model and validated the antagonistic effect of c-MYC on AR-targets in patient samples. We found that c-Myc overexpression partially reprogrammed AR chromatin occupancy and was associated with altered histone marks distribution, most notably H3K4me1 and H3K27me3. We found c-Myc and the AR co-occupy a substantial number of binding sites and these exhibited enhancer-like characteristics. Interestingly, c-Myc overexpression antagonised clinically relevant AR target genes. Therefore, as an example, we validated the antagonistic relationship between c-Myc and two AR target genes, KLK3 (alias PSA, prostate specific antigen), and Glycine N-Methyltransferase (GNMT), in patient samples. Our findings provide unbiased evidence that MYC overexpression deregulates the AR transcriptional program, which is thought to be a driving force in PCa.

1. Introduction

Prostate cancer (PCa) is the most common non-cutaneous cancer in men and the second most common cause of cancer-related deaths. Genomic alterations and changes in transcriptional regulation are keys to PCa initiation and progression and a crucial factor is dysregulated androgen receptor (AR) activity (Barfeld et al., 2014a). The AR is a ligand-activated transcription factor that controls key cellular processes including anabolic metabolism and cell cycle control (Barfeld et al., 2014b; Massie et al., 2011). Despite AR-targeted therapies, most

advanced cases of PCa still maintain an active AR signaling network, presumably due to a range of activating mutations, gene amplifications and splicing events (Hu et al., 2012; Robinson et al., 2015; Taylor et al., 2010). Notably, genomic alterations affecting the AR directly appear to be limited to late stages of PCa (Taylor et al., 2010).

On the other hand, various other oncogenic signaling pathways and transcription factors are commonly mutated or amplified early in PCa. These include a) hyperactivation of the phosphoinositide 3-kinase (PI3K) pathway, b) translocations and fusions of a range of ETS transcription factors, such as ERG or ETV1, which place these factors under control of the AR, and c) amplification or overexpression of the oncogenic transcription factor c-Myc (MYC) (Robinson et al., 2015; Taylor et al., 2010).

The chromosome region containing the MYC gene (8q24) is commonly amplified in PCa, and several reports have confirmed elevated levels of MYC mRNA and protein in PCa patients (Gurel et al., 2008; Jenkins et al., 1997). Mechanistically, the work on MYC in PCa confirms its contribution to ribosome biogenesis and metabolism (Barfeld et al.,

2015; Koh et al., 2011a). Whilst other transcription factors, such as ERG or ETV1, have been shown to antagonize and amplify AR-mediated transcriptional activity, respectively (Baena et al., 2013; Yu et al., 2010), the relationship between the AR and MYC in PCa is yet to be explored in detail. Therefore, in this study we mapped the genome-wide chromatin binding sites for MYC and AR in PCa cells and evaluated the effect of MYC overexpression on AR chromatin occupancy and transcriptional output. Developing a clearer understanding of the interplay between transcription factors in PCa is important in defining the correct context for biomarkers and therapeutic targets.

2. Materials and Methods

2.1. Cell Culture and Manipulation

The LNCaP-MYC (Ramos-Montoya et al., 2014) and the corresponding empty vector (EV) line were cultured at 37 °C and 5% CO$_2$ in RPMI1640 (Gibco, 21875), containing 10% fetal bovine serum (FBS) (Gibco, 10500) and 2 μg/ml puromycin and 200 μg/ml G418 (Gibco, 10131019) for plasmid maintenance. For hormone starvation, cells were washed once with PBS (Gibco, 10010) and cultured in phenol red-free RMPI1640 (Gibco, 11835063), containing 10% charcoal-stripped FBS (Gibco, 12676029) for 72 h before starting the experiment. MYC overexpression was induced using 2 μg/ml doxycycline. Parental LNCaP cells were cultured under the same conditions minus the antibiotics. VCaP cells were cultured in DMEM (Gibco), containing 10% FBS under the same conditions.

For viability assays, the amount of viable cells was determined using Cell Aequous solution MTS reagent (Promega, G3581) following the manufacturer's recommendations.

Sarcosine levels were determined using a Sarcosine Assay Kit (Abcam, ab65338) following the manufacturer's recommendations.

Reverse siRNA transfection was performed using the Lipofectamine RNAiMAX transfection reagent (Life technologies, 13778150) and OptiMEM transfection medium (Life technologies, 31985-070). The following siRNAs were used: ON-TARGETplus Non-Targeting Pool (Thermo Scientific, D-001810-10) and ON-TARGETplus Human MYC SMARTpool (Thermo Scientific, L-003282-02).

2.2. ChIP-exo/-seq and Analysis

ChIP-exo and ChIP-seq were performed as previously described (Massie et al., 2011; Serandour et al., 2013). Antibodies used were AR (scbt, sc-816x), MYC (R&D, AF3696), H3K4me1 (Diagenode, pAb-194-050), H3K4me3 (Diagenode, C154100003), H3K27ac (Diagenode, pAb-196-050), H3K27me3 (Diagenode, pAb-195-050) and IgG control (scbt, sc-2027). Briefly, cultured LNCaP MYC cells were crosslinked, quenched, lysed and the chromatin sheared to an average size of approximately 200–300 bp. Following overnight incubation with specific antibodies or an IgG control, several on-bead enzymatic reactions including two exonuclease digestions were performed prior to overnight crosslink reversal and elution. DNA was cleaned-up and subjected to final enzymatic reactions. The resulting Illumina-compatible libraries were single-end sequenced on Illumina HiSeq 2000 instruments (Illumina). For ChIP-seq experiments, Illumina libraries were prepared using the TruSeq kit and single-end sequenced on Illumina HiSeq 2000 instruments (Illumina), as previously described (Massie et al., 2011).

The raw reads were aligned using novoalign (http://www.novocraft.com) or bowtie (for histone ChIPs) with default parameters on the human genome version 19 (hg19). Filter to SAM quality 20 was applied and only a maximum of 5 duplicated reads were kept. The peak detection (i.e. binding site detection) was performed using MACS with default parameters using inputs samples as controls (Zhang et al., 2008). Only reproducible peaks (i.e. those that occurred in both replicates) were considered in downstream analyses.

To assess the presence of motifs of other transcription factors in the ChIP-exo or ChIP-seq dataset, we looked for overrepresented TF motifs using "findMotifsGenome.pl", and peaks distribution analysis with annotatePeaks.pl, both parts of the HOMER package. Read distribution analysis was performed using an in-house script (Urbanucci et al., 2012), which generated a matrix of "normalized differences between coverage integrals in treated versus control samples aligned reads" using a 2000 bp window around peaks. Normalization was computed as 10 M/dataset size. Other downstream analyses were performed using the Galaxy platform and the CEAS package.

To obtain the MYC binding profile which we called "MYC ENCODE compendium", we created a custom bed file containing MYC peaks present in any of the following cell lines used by the ENCODE (Consortium, 2004) (https://genome.ucsc.edu/): HeLa, H1-ESC, K562, HepG2 and HUVEC.

2.3. Quantitative Real Time PCR (qRT-PCR) and ChIP qPCR

Total RNA was isolated using the Qiagen RNeasy kit (Qiagen, 74106) following the manufacturer's recommendations. RNA concentration and purity was measured using a NanoDrop instrument (Thermo Scientific). 500 ng to 1 μg total RNA were reverse transcribed using the Super-Script VILO kit (Applied Biosystems, 11754) following the manufacturer's recommendations. qRT-PCR was performed using SYBR green master mix (Applied Biosystems, 4385612). Amplification was performed in duplicate series using the ABI 7900HT FAST Sequence Detection System (Applied Biosystems) with the following cycling conditions, 50 °C for 2 min, 95 °C for 10 min, 40 cycles of 95 °C for 15 s and 60 °C for 60 s. Transcript levels were normalized to vehicle controls and the expression levels of beta-actin using the 2^ddCt method. A complete list of primers can be found in Table S1.

2.4. Expression Arrays and Analysis

For microarray analysis, RNA integrity was confirmed using a 2100 Bioanalyzer (Agilent) and Total RNA Nano Chip (Agilent, 5067–1511). 500 ng RNA were reverse transcribed and Biotin-labeled using the TotalPrep-96 RNA Amplification kit (Illumina, 4393543) following the manufacturer's recommendations. Resuspended cRNA samples were hybridized onto Human HT-12 Expression BeadChips (Illumina, BD-103-0204). Missing probes were imputed using Illumina's GenomeStudio Gene Expression Module. The imputed probe datasets were analyzed using the freely available J-Express 2012 software (http://jexpress.bioinfo.no/site/). The raw data was quantile normalized and log2 transformed prior to analysis. Differential expression analysis was performed using the grouped triplicate experiments and Rank product analysis. Probes with a q-value of <0.1 were considered significantly up- or downregulated. For hierarchical clustering using complete linkage and Pearson correlation, differentially expressed probes were merged and high level mean and variance normalized. Heatmaps were drawn using Java treeview.

Gene Set Enrichment Analysis (GSEA) is a bioinformatic method that is used to assess whether sets of genes are significantly different. The method computes the similarity between a query gene-set compared to the gene-sets available in the GSEA database and derived from published studies. For GSEA, the javaGSEA Desktop Application (http://www.broadinstitute.org/gsea/index.jsp) was used with the following gene set collections: c2: curated gene sets. An additional dataset was included in the analysis for the purpose of this study: an AR signature derived from Asangani et al. (Asangani et al., 2014).

KEGG and GO pathway analyses were performed using the genecodis tool (http://genecodis.cnb.csic.es/) (Carmona-Saez et al., 2007).

To identify statistically significant biochemical recurrence courses, recursive partitioning was performed on a single gene expression profile using the 'party' package from CRAN (Han et al., 2012) with

accompanying biochemical recurrence data taken from (Glinsky et al., 2004; Taylor et al., 2010). Kaplan Meier plots of the risk of biochemical recurrence were produced using the 'survival' package and p-values from the log rank test were corrected using the Bonferroni correction method.

2.5. Western Blotting

Cells were trypsinized and washed with cold PBS prior to resuspension in RIPA lysis buffer (30 mM Tris-HCl, 150 mM NaCl, 1 mM EDTA, 0.5% NP40, 0.1% Na-deoxycholate, 0.1% SDS, pH 7.4) supplemented with protease inhibitors (Roche, 11873580001), rotated at 4 °C for 10 min and sonicated in a Bioruptor NextGen (Diagenode) at maximum power for ten cycles of 30s ON, 30s OFF to break nuclei and other cellular structures. Lysates were centrifuged for 10 min at 18,000 g and 4 °C and the supernatant transferred to a new tube. Protein concentration was determined using a BCA assay (Pierce, 23227) and equalized with RIPA buffer. Extracts were mixed with LDS NuPAGE buffer (Life technologies, NP0008) and Sample Reducing Agent (Life technologies, NP0009) and denatured for 10 min at 70 °C. Equal amounts were loaded onto 4–12% gradient Bis-Tris NuPAGE gels (Life technologies, NP0323). Separated proteins were semi-dry blotted using the iBlot Gel Transfer Device (Life technologies). Membranes were blocked in 5% BSA (Sigma, A2153) in TBS with 0.1% Tween-20 (Sigma, P5927) for 1 h prior to overnight incubation with appropriate concentrations of primary antibodies. The next day, membranes were washed with TBS with 0.1% Tween-20 and incubated with appropriate secondary antibody for 1 h at room temperature. After washing with TBS with 0.1% Tween-20, membranes were developed using the Novex ECL Reagent kit (Life technologies, WP20005) or a super-sensitive HRP substrate (Rockland, FEMTOMAX-110). Primary antibodies used were MYC (Abcam, ab32072), KLK3 (Dako, A0562), CAMKK2 (Sigma, HPA017389), GNMT (R&D, AF6526), actin (Cell Signaling, 2118S) and GAPDH (Cell Signaling, 5125S). Secondary HRP-conjugated anti-rabbit and anti-goat were purchased from Dako (P0448 and P0449, respectively).

Densitometry analysis was performed using the freely available software ImageJ and protein levels normalized to b-actin/GAPDH. For the purpose of this study, a validation of MYC antibody is shown in Fig. S7d upon MYC knockdown.

2.6. Rapid Immunoprecipitation Mass Spectrometry of Endogenous Proteins (RIME)

To perform the RIME we used MYC (Abcam, ab32072), and AR (N-20) sc-816 SantaCruz. The RIME procedure has been previously described (Mohammed et al., 2013; Mohammed et al., 2016).

2.7. Co-immunoprecipitation

The same antibodies utilized for RIME were also used for Co-IP as previously described (Itkonen and Mills, 2013).

2.8. Immunohistochemistry – Tissue Microarray

For this study we used a total of 352 samples, of which 68 were benign prostatic hyperplasia (BPH), 101 primary tumours without lymph node metastases, 71 primary tumours with lymph node metastases and 112 transurethral resections of castration-resistant prostate cancer (CRPC) samples. Specimens were obtained from the Vancouver Prostate Centre Tissue Bank. H&E slides were first reviewed and desired areas were marked also on their correspondent paraffin blocks. 3 TMAs were manually constructed (Beecher Instruments, MD, USA) by punching duplicate cores of 1 mm for each sample. All the specimens were from radical prostatectomy except 12 CRPC samples that obtained from transurethral resection of Prostate (TURP).

Immunohistochemical staining was performed using the Ventana autostainer model Discover XT™ (Ventana Medical System, Tuscan, Arizona) with enzyme labeled biotin streptavidin system and solvent resistant Red Map kit by using MYC (Abcam, ab32072), KLK3 (Sigma, HPA000764), and GNMT (scbt, sc-68871) antibodies. The antibody against GNMT was previously validated (Khan et al., 2013).

The scoring method used was based on assigning a value on a four-point scale to each immunostain. Descriptively, 0 represents no staining by any tumor cells (negative), 1 represents a faint or focal, questionably present stain (weak), 2 represents a stain of convincing intensity in a minority of cells (moderate), and 3 a stain of convincing intensity in a majority of cells (strong). For MYC, nuclear staining intensity was calculated as the product of "fraction of positive nuclei" and staining intensity.

2.9. Immunohistochemistry - Dual Staining for c-Myc and PSA in Individual Tissue Sections

Tissue sections were obtained from the Johns Hopkins biorepository under appropriate research ethics approval. Tissue slides were deparaffinized and hydrated. Slides were preheated to melt the paraffin at 60 °C for ten minuutes and xylene and alcohol used to prime them for hydration in distilled water. The slides were then deparaffinized for antigen retrieval by steaming for 45 min in EDTA. Myc staining was then performed using a DAKO signal amplification kit as previously described (Gurel et al., 2008) with the primary antibody (Abcam) used at 1:4000 dilution in an overnight incubation at 4 °C. Myc staining was ultimately resolved with using Vector ImmPACT RED (SK-5105) in a 30 min incubation. Following this PSA staining was performed on the same section using a mouse PSA primary antibody (Dako) at a 1:50 dilution for 45 min at room temperature and staining was visualised using a Power Vision Poly-HRP anti-Mouse IgG also as previously described. This generated a two-colour stained tissue section in which c-Myc was red and PSA was brown and areas of the section were qualitatively evaluated for mutual exclusivity of stain.

2.10. Statistics

Unless stated otherwise, mean values with standard error of the mean (SEM) are displayed and significance was confirmed using paired two-tailed Student's t-test. *$p < 0.05$, **$p < 0.01$, ***$p < 0.001$, ****$p < 0.0001$.

2.11. Availability of supporting data

The datasets supporting the results of this article are available in the NCBI GEO data repository (GSE73995).

3. Results

3.1. Androgen-treatment of Hormone-deprived Prostate Cancer Cells Reduces MYC Levels

Elevated MYC levels are a common hallmark of PCa and both amplification (Jenkins et al., 1997) and overexpression (Gurel et al., 2008) have been reported. Recently, it was shown in apocrine breast cancers that MYC mRNA and protein levels, as well as transcriptional activity are enhanced by androgen treatment and concomitant activation of the AR (Ni et al., 2013). LNCaP and VCaP cell lines are two commonly used androgen responsive PCa models expressing both AR and MYC. Given the many similarities between hormone-dependent breast and prostate cancers, we firstly treated hormone-deprived LNCaP and VCaP PCa cell lines with the synthetic androgen R1881 using a commonly used concentration (1 nM). In stark contrast to the apocrine breast cancer cell line MDA-MB-453 (Ni et al., 2013), we did not observe an increase of MYC mRNA and protein but the opposite; both MYC mRNA

and protein levels were reduced after 12 h of R1881 treatment and remained downregulated for up to 24 h (Fig. 1a–b). This implied an antagonistic relationship between these two transcription factors.

We then sought to test whether this extends to effects on chromatin occupancy and gene expression. Thus, we used a recently developed stably transfected LNCaP line (LNCaP-MYC) that inducibly overexpresses MYC (Barfeld et al., 2015). Upon treatment with 2 μg/ml doxycycline, *MYC* mRNA increases about 8-fold and MYC protein roughly 3-fold (Barfeld et al., 2015). These levels are approximately in line with previously reported increases of *MYC* mRNA and protein in clinical samples of PCa compared to normal tissue controls (Gurel et al., 2008). MYC overexpression has previously been reported to confer androgen-independent growth in prostate epithelial cells (Bernard et al., 2003), and we confirmed this effect in our cell line by inducing MYC overexpression with doxycycline in steroid-deprived conditions on a time course up to 72 h (Fig. S1a). Comparable effects on viability

were observed with androgen treatment (R1881). However, the combination with doxycycline did not produce a further viability enhancement.

3.2. ChIP-exo of AR and MYC Reveals Partially Overlapping Binding Patterns of Both Transcription Factors

Firstly, we performed a modified ChIP-seq protocol (ChIP-exo) for MYC and the AR to generate genome-wide site maps (Fig. S1b). ChIP-exo incorporates an exonuclease digestion to improve the spatial definition of the resultant peaks (Serandour et al., 2013). LNCaP-MYC cells were hormone-deprived for 72 h and treated for 16 h with 1 nM R1881 or 1 nM R1881 plus 2 μg/ml doxycycline to induce MYC overexpression. This time point was chosen to make the ChIP-exo datasets comparable to published ChIP-seq datasets (Yu et al., 2010), and was also a time point at which doxycycline treatment achieved increased
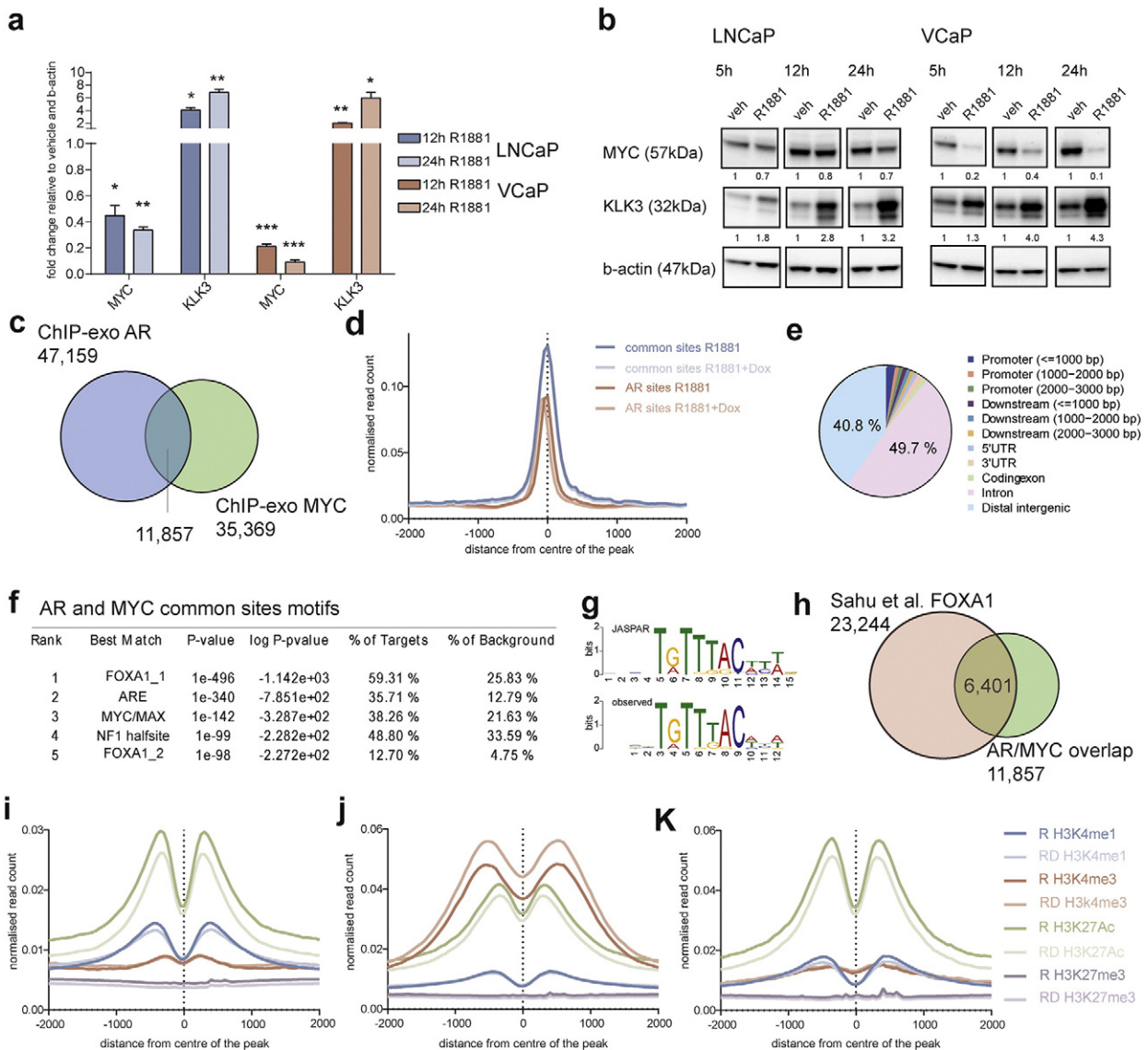

Fig. 1. AR and MYC are co-enriched at enhancer-like binding sites. (a–b) LNCaP and VCaP cells were hormone-starved for 72 h and subsequently treated with 1 nM R1881 for the indicated time. (a) Transcript and (b) protein levels of MYC and KLK3 relative to b-actin were measured by real-time PCR and Western blotting analysis, respectively (n = 3). (c) Venn diagram showing the overlap between MYC and AR binding sites in LNCaP-MYC cells. (d) Density plot of AR ChIP-exo reads within ±2 kb of common AR/MYC binding sites or all AR binding sites in LNCaP-MYC cells treated with R1881 orR1881 + doxycycline. (e) Distribution of common AR/MYC sites in LNCaP-MYC cells across the genome. (f) Motif analysis of common AR/MYC binding sites in LNCaP-MYC cells. The top 5 motifs are shown. (g) Sequence logo of the top motif for FOXA1 in the JASPAR database and as observed in this study. (h) Venn diagram showing the overlap between common AR/MYC binding sites in LNCaP-MYC and FOXA1 binding sites in LNCaP derivatives retrieved from a previously published dataset (Sahu et al., 2011). Density plots of H3K4me1, H3K4me3, H3K27ac and H3K27me3 ChIP-seq reads within ±2 kb of (i) AR, (j) MYC and (k) common AR/MYC binding sites in LNCaP-MYC treated with R1881 (R) or R1881 + doxycycline (RD).

MYC protein levels and had a profound impact on gene expression. The overlap between our biological replicates ranged from 60 to 90% and we selected peaks that were conserved in both replicates for all subsequent downstream analysis steps (Fig. S1c). We previously demonstrated that overexpressing AR in LNCaP cells enhanced the ability of AR to bind chromatin (Urbanucci et al., 2012). Overexpression of MYC, however, did not increase the number of its binding sites dramatically (27,556 peaks under R1881 treatment and 28,996 peaks when doxycycline was added to overexpress MYC) (Fig. S1d). A large proportion of MYC peaks were conserved in both conditions but 7339 peaks were lost (26%) and 8856 gained (32%) (Fig. S1d). Notably, however, MYC overexpression did not have a significant effect on overall number of sequence reads recovered at MYC binding sites, which reflects the intensity of chromatin binding (Fig. S1e). Furthermore, the lost and gained sites were of low affinity compared to the overlapping sites (Fig. S1f). Taken together, these data suggest that MYC overexpression does not dramatically alter MYC binding to the chromatin.

Other studies on AR modulators, such as TMPRSS2-ERG or FOXA1, have assessed impacts of these factors on both the number and distribution of AR sites (Sahu et al., 2011; Yu et al., 2010). Consequently, we went on to assess the impact of MYC overexpression on AR recruitment and found 37,288 AR peaks without overexpression and 41,505 peaks with MYC overexpression, an increase of about 11% (Fig. S1f). Furthermore, MYC overexpression resulted in a partial reprogramming of the AR with 5391 AR binding sites lost (14%) and 10,396 sites gained (27%) (Fig. S1f). However, MYC overexpression did not alter the number of sequence reads recovered at AR binding sites and the lost/gained sites appeared to be low affinity binding sites (Fig. S1g). Thus, MYC overexpression did not dramatically change AR-binding patterns.

The overlaps between our AR ChIP-exo and published AR ChIP-seq studies ranged from 57 to 81% (Fig. S1h). To assess the quality of our MYC dataset, we compared it to a number of published MYC ChIP-seq datasets generated by ENCODE (Consortium, 2004) (see Supplementary material for details). The overlap between the consensus sites of the LNCaP-MYC dataset generated in this study, and the "MYC ENCODE compendium" was >82% (Fig. S1h). MYC binding sites were, as previously reported in other cell types, significantly promoter proximal (amounting to around 30% of mapped sites) (Fig. S1i). By contrast, and also in keeping with previous studies (Massie et al., 2011; Yu et al., 2010), there were only around 5% of AR sites that were promoter proximal (Fig. S1i). Motif enrichment at the MYC binding sites yielded MYC/MAX as the most enriched motif followed by FOXA1, ELK4, CTCF and NRF1 (Fig. S1j). ELK4 is a member of the ETS family of transcription factors, which also contains ERG, and Yu et al. reported ERG to be predominantly associated with promoters (Yu et al., 2010). Motif enrichment on the AR sites yielded androgen response elements (ARE) followed by forkhead family transcription factors (FOXA1, FOXO1 and FOXA2) and HOXD13 motifs (Fig. S1k). The significant enrichment of motifs for the Forkhead family of transcription factors within AR binding sites is in-line with previously published data (Wang et al., 2007), whilst the motif enrichment for FOXA1 consensus sequences within MYC sites has not been reported previously.

Having observed no notable changes in MYC or AR binding upon MYC overexpression, we then focused on the AR/MYC overlapping sites, which amounted to roughly 25% of all AR sites and 30% of all MYC sites (Fig. 1c). The average normalized read count for AR/MYC overlapping sites was approximately 50% higher than that for all AR binding sites, suggesting that AR/MYC overlapping sites are high-affinity AR binding sites (Fig. 1d). The site distribution for the AR/MYC overlapping sites mirrored that of the total pool of AR sites, with mainly an intergenic and intronic pattern and with only around 5% of sites promoter proximal (Fig. 1e). The motif enrichment observed for these overlapping sites was a combination of the significantly enriched motifs found in the AR and MYC sites alone, in other words featuring FOXA1, ARE and MYC/MAX (Fig. 1f–g). FOXA1 is the most extensively studied AR coregulator and we were able to validate the prediction of

enrichment made in the motif analysis by downloading and using an experimental dataset, FOXA1 ChIP-seq data generated in LNCaP derivatives (Sahu et al., 2011), which showed a 53% overlap between FOXA1 and AR/MYC common sites (Fig. 1h). Although this remains to be experimentally tested, these data suggest that AR and MYC may share a common pioneer factor in PCa cells. This has been shown for the estrogen receptor and AR (Hurtado et al., 2011; Lupien et al., 2008; Sahu et al., 2011; Wang et al., 2011a). In support of this hypothesis, a recent study by Jozwik et al. found that FOXA1 guides chromatin modifiers to genes regulatory regions, and therefore may be responsible for effects on transcription mediated by multiple TFs, not only nuclear receptors but also others such as MYC (Jozwik et al., 2016).

3.3. MYC Overexpression Alters Global H3K4me1 and H3K27me3 Levels

It has previously been shown that global H3K27me3 levels correlate with differentiation and are inversely correlated with MYC (Pellakuru et al., 2012). In other studies, an enzyme required for generating H3K27me3 marks, enhancer of zeste 2 polycomb repressive complex 2 subunit (EZH2), has been reported to be overexpressed in PCa, to function as an AR coactivator and to be a MYC target gene (Koh et al., 2011b; Varambally et al., 2002). Furthermore, the antagonistic effect of TMPRSS2-ERG on the AR has been shown to be mediated by EZH2 and concomitant changes in H3K27me3 (Yu et al., 2010). To assess whether MYC overexpression in our cell line model would affect histone mark patterns, we generated ChIP-seq data for H3K27me3 as well as histone marks reflective of active promoters (H3K4me3) and enhancers (H3K4me1) and of active enhancers/promoters (H3K27ac) under the same conditions as for our AR and MYC ChIP-exo datasets (Ernst et al., 2011). To assess the comparability of our data with published studies, we downloaded ChIP-seq data generated in LNCaP for these histone marks (Wang et al., 2011a; Yu et al., 2010). Despite differences in the treatment conditions, we observed substantial overlaps between our data and those from these published studies with overlaps ranging from 45 to 100% (Fig. S2a). Furthermore, the genome-wide distribution of these histone marks in our datasets mirrored that of the published datasets and the general expected distribution for these marks based on their confirmed promoter and enhancer associations – for example 18–24% (our data compared to Wang et al. (Wang et al., 2011a)) of H3K4me3 sites were present at proximal promoters (Fig. S2b). The most significant effects of MYC overexpression were on H3K27me3 and H3K4me1 marks for which there was a 21% increase in the number of peaks in the former case upon doxycycline treatment and a 5% decrease in the number of sites in the latter case (Fig. S2c). This was also reflected in the relative normalized read counts of lost and gained sites in these treatment conditions (Fig. S2d).

We then integrated the histone mark data with the AR and MYC datasets and found that the AR sites had enhancer-characteristic histone marks (H3K4me1 and H3K27ac) (Fig. 1i). On the other hand, MYC sites had promoter-characteristic histone marks (H3K4me3 and H3K27ac) (Fig. 1j). Notably, AR/MYC overlapping sites exhibited the same enhancer characteristics as pure AR binding sites (Fig. 1k), which suggested that AR and MYC co-occupy a substantial amount of enhancers. Despite the increased number of H3K27me3 peaks upon MYC overexpression, we observed no substantial association of H3K27me3 with AR/MYC sites (Fig. 1i–k). We also undertook extensive characterization of the relations between AR and MYC at such enhancers using rapid immuno-precipitation mass spectrometry of endogenous proteins (RIME) (Mohammed et al., 2016) and co-immunoprecipitation (Fig. S3 and Table S2). Although we were able to retrieve well known interactors of AR, such as HOXB13 (Jung et al., 2004; Kim et al., 2010), and MYC, such as MAX (Kato et al., 1992) and TRRAP1 (McMahon et al., 1998), we were not able to retrieve any evidence of direct interaction between the AR and MYC. Interestingly MYC and AR shared interactor proteins linked to DNA replication (MCM3) (Alvarez et al., 2015; Gibson et al., 1990; Madine et al., 1995; McMahon et al., 1998) and repair pathways

(RAD50) (Dolganov et al., 1996; Paull et al., 2000) (Fig. S3c). Therefore, we sought to understand the biological significance of the interplay between MYC and AR in relation to these processes. Interestingly, we found that overexpressing MYC, PCa cells show increased DNA damage measured as phosphorylation of H2A.X (Fig. S4a). The increased DNA damage effect however is independent of androgens levels to which PCa cells are exposed, and the overexpression of c-MYC only confers growth advantage when cells are grown in absence of androgens (Fig. S1a), as previously reported (Gao et al., 2013; Kokontis et al., 1994). This suggests that the AR signaling plays a role in masking such effect. In fact, cells growing in presence of androgens do not display a growth advantage when MYC is overexpressed (Fig. S4b). We previously showed that MYC is overexpressed in the majority of CRPCs (Gurel et al., 2008). Therefore the tendency to upregulate AR signaling in advanced tumours, which is a well-known hallmark of progression (Waltering et al., 2012), may be driven by the need to overcome DNA damage produced in these cells in consequence of MYC upregulation. These data are also in full agreement with the same reports showing direct upregulation of c-MYC by AR overexpression when PCa cells adapt to grow in castrate conditions (Gao et al., 2013; Kokontis et al., 1994; Waltering et al., 2009) or, more specifically, when they are defined to display AR ligand independent cell growth (Gao et al., 2013).

3.4. MYC Overexpression Antagonises AR-mediated Transcriptional Output

Next, we assessed the effects of MYC overexpression on transcriptional output upon androgen treatment. It has previously been reported in apocrine breast cancer cells that MYC can act as a transcriptional amplifier of AR target genes (Ni et al., 2013). To assess whether MYC exerts similar functions in PCa cells, we performed expression microarrays upon hormone-deprivation for 72 h and treatment for 5 h and 12 h with 1 nM R1881 or 1 nM R1881 plus 2 μg/ml doxycycline to capture primarily direct target genes of both the AR and MYC.

Unbiased Gene Set Enrichment Analysis (GSEA) using "c2: curated gene sets" and genes that were deregulated upon 12 h of R1881 treatment as input, revealed NELSON_RESPONSE_TO_ANDROGEN_UP (Nelson et al., 2002) as the most significantly enriched (Fig. 2a and Table S3). The same analysis but using genes deregulated by the combination of MYC overexpression and R1881 treatment, led to a significant enrichment of established MYC target genes as the SCHUHMACHER_MYC_TARGETS_UP (Schuhmacher et al., 2001) gene set was the top enriched (Fig. 2a). These data confirms the validity of the LNCaP-MYC model for subsequent analyses. Surprisingly, the top-ranked downregulated gene set upon MYC overexpression was NELSON_RESPONSE_TO_ANDROGEN_UP (Nelson et al., 2002), suggesting that MYC rather antagonises than amplifies AR-induced gene expression in PCa cells (Fig. 2a). We also used another established AR target gene signature by Asangani et al. (Asangani et al., 2014) in GSEA and found that the pattern was identical to that observed on the Nelson signature (Fig. 2a). These findings were further corroborated by reanalysed data from a previously published study where siRNA-mediated depletion of MYC in combination with expression microarrays revealed MYC's role as a driver of ribosome biogenesis and nucleolar alterations (Koh et al., 2011a). GSEA revealed NELSON_RESPONSE_TO_ANDROGEN_UP to be the top upregulated gene set upon MYC-downregulation (Fig. 2b and Table S3), which confirmed MYC's repressive function.

On an individual gene level, the repressive impact of MYC overexpression measured at both 5 h and 12 h amounted to roughly 25% of androgen-induced genes whilst only around 1.5% of androgen-induced genes were further increased in expression when MYC levels were elevated (Fig. 2c–f and Table S4). Interestingly, this 1.5% included inosine monophosphate dehydrogenase, which we have previously characterised as a drug target that enhances response to anti-androgens (Barfeld et al., 2015). We subjected AR targets that were antagonised by MYC overexpression to gene ontology (GO) and Kyoto Encyclopedia of

Genes and Genomes (KEGG) pathway analysis and observed classifications ranging from positive regulation of transcription by RNA polymerase II through to various metabolic pathways, including the UDP-N-acetylglucosamine biosynthetic process (Fig. S5). Interestingly, MYC has previously been reported to enhance RNA polymerase II processivity (Rahl et al., 2010), and the UDP-N-acetylglucosamine biosynthetic process has been shown to influence MYC stability and is a critical component of a novel discriminatory signature capable of subclustering patients into different disease stages (Barfeld et al., 2014a; Itkonen et al., 2013).

3.5. Prostate Cancer Biomarkers are Antagonised by MYC Overexpression

So far we have established that the relationship between androgen-dependent AR activation and MYC overexpression is predominantly antagonistic, featuring repression of AR target genes. These included multiple established AR target genes, such as KLK3 and CAMKK2, and these exhibited overlapping AR/MYC binding within a 50 kb window, as well as TSS-associated MYC peaks (Fig. 3a–b). We validated the antagonistic relationship between AR and MYC for a number of genes from the microarray experiment. We selected KLK3, CAMKK2, ERRFI1, SOCS2 and GNMT, which reflected previously published PCa biomarkers and/or therapeutic targets (Khan et al., 2013; Massie et al., 2011; Zhu et al., 2013). We confirmed AR and MYC recruitment to sites associated with CAMKK2, SOCS2, ERRFI1, KLK3 and GNMT using ChIP-qPCR based on our data (Fig. 3c–d and Fig. S6). Using qRT-PCR, we confirmed repression of the transcripts (Fig. 3e). Conversely, siRNA-mediated depletion of MYC increased the mRNA levels of some but not all of these genes in LNCaP and VCaP cells (Fig. 3f), suggesting that context specificity, such as the relative levels of AR and MYC in the two different cell lines, might play a crucial role. Additionally, Western blotting showed that MYC overexpression repressed GNMT, CAMKK2 and KLK3 at the protein level in LNCaP-MYC cells (Fig. 3g). Notably, these genes were not repressed by doxycycline in the corresponding empty vector cell line (LNCaP-EV), which ruled out a doxycycline effect (Fig. S7a–b). Sarcosine is the metabolite produced by GNMT and it has previously been reported to be a putative marker of aggressive PCa and increased invasiveness (Sreekumar et al., 2009). Thus, we measured sarcosine levels in LNCaP-MYC cells. Interestingly, we found that MYC overexpression reduced the total levels of intracellular sarcosine compared to cells treated with R1881 alone (Fig. S7c). These data are in accordance with a few reports that have failed to validate sarcosine as a marker of aggressive PCa (Jentzmik et al., 2010; Lima et al., 2016). Furthermore, subsets of PCa can progress after treatment without PSA recurrence (Lee et al., 2010; Sella et al., 2000). Therefore, whilst it is important to acknowledge that the AR and AR-driven genes and metabolites are markers of aggressive disease, this is not true for all patients. Our data shows that in those patients for which sarcosine is not effectively predictive, the scarce efficacy may reflect a dominant effect on gene expression from c-Myc versus the AR, which affects GNMT expression.

3.6. MYC is Inversely Correlated with GNMT and KLK3 in Prostate Cancer Patients

AR target genes have long been proposed as PCa biomarkers and some have been shown to perform in opposite and contradictory directions in independent cohort studies. Examples of this include SOCS2 (Hoefer et al., 2014; Zhu et al., 2013) and GNMT (Huang et al., 2007; Khan et al., 2013). One possible explanation for these observations is that the direction of the association reflects the dominant transcription factor/oncogene (e.g. MYC or AR) in the cohort. Improving our contextual understanding of the drivers of gene expression of PCa is therefore critical to appropriately position biomarkers. In order to assess the clinical relevance of induced AR target genes that were antagonised by MYC, we tested the individual prognostic value of these 166 genes in two published datasets (Glinsky et al., 2004; Taylor et al., 2010).
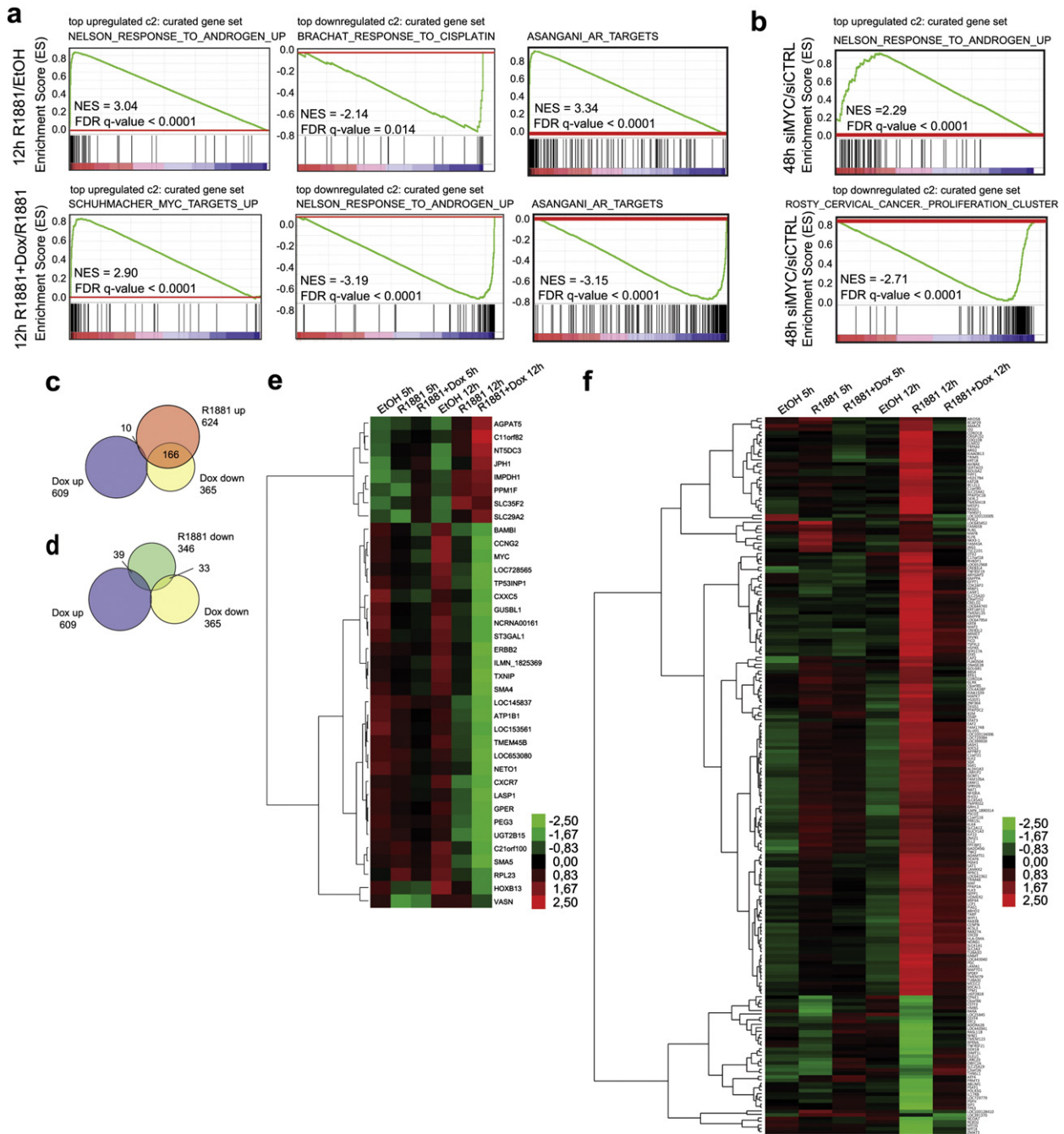
Fig. 2. MYC overexpression antagonises R1881-induced gene expression. (a) Gene Set Enrichment Analysis (GSEA) of hormone-starved LNCaP-MYC cells treated with R1881 (top row) or R1881 + doxycycline (bottom row) for 12 h. The c2: curated gene set compendium and a custom AR target gene signature consisting of genes upregulated by hormone treatment in both LNCaP and VCaP cells from Asangani et al. (Asangani et al., 2014) were used as input. The top up- and downregulated gene sets of the c2 compendium are shown. (b) GSEA of MYC-depleted LNCaP using the c2: curated gene set compendium as input. The top up- and downregulated gene sets are shown (Koh et al., 2011a). Venn diagrams showing (c) overlaps between R1881-induced genes and genes altered by MYC-overexpression, and (d) R1881-repressed genes and genes altered by MYC-overexpression. Heatmap of unsupervised hierarchical clustering for R1881-induced and -repressed genes for which MYC overexpression (e) enhanced or (f) antagonised AR action.

Fourteen induced AR targets (8%) antagonised by MYC overexpression predicted a shorter time to biochemical recurrence when their expression levels were low in two independent datasets (Fig. 4a and Table S5). These included Suppressor Of Cytokine Signaling 2 (SOCS2) (Fig. 4b), Krueppel-like factor 6 (KLF6) (Fig. 4c), and ELL-associated factor 2 (EAF2) (Fig. 4d). KLF6 loss of function has previously been implicated in resistance to androgen deprivation (Liu et al., 2012), and EAF2 is a putative tumor suppressor and apoptosis inducer (Xiao et al., 2003).

Next, we sought to assess the relationship between MYC and the two antagonised AR targets KLK3 and GNMT in PCa tissue using immunohistochemistry and tissue microarrays (TMA). Our TMA contained a total of

352 cases, of which 68 were benign prostatic hyperplasia (BPH), 101 primary tumours without lymph node metastases, 71 primary tumours with lymph node metastases and 112 transurethral resections of castration-resistant prostate cancer (CRPC) samples. MYC nuclear staining was increased in CRPC and conversely, the staining intensities for KLK3 and GNMT were decreased (Fig. 4e–j and Fig. S8 and S9a–d). Furthermore, we performed double-labelling of PCa cases using antibodies against MYC and KLK3 to show the inverse correlation on a single cell level (Fig. S9e–f). In 4 of 5 cases, carcinoma lesions contained a number of areas with inverse levels of MYC and KLK3; (i.e. there were areas with high staining for MYC protein in nuclei that exhibited correspondingly
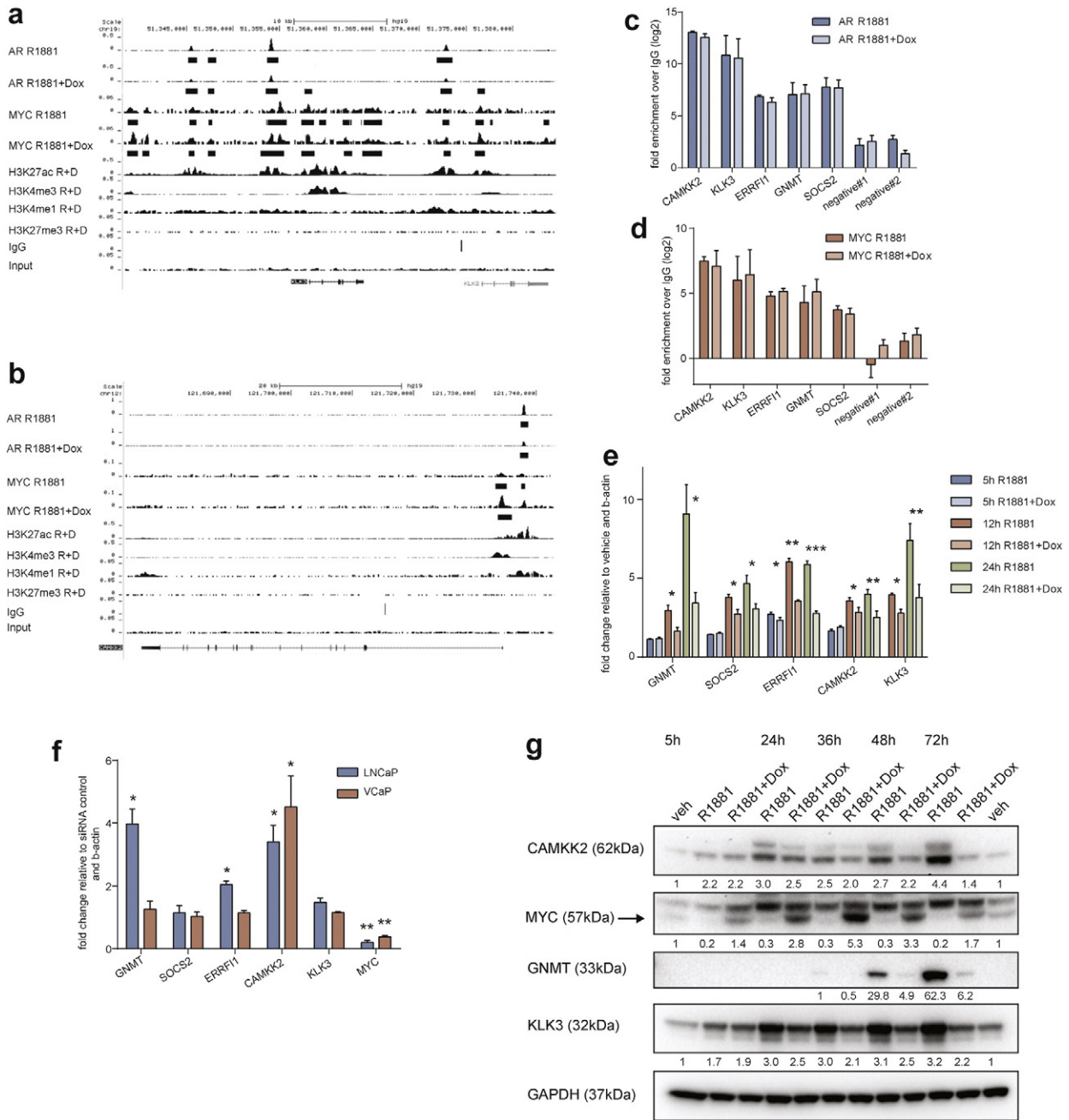
Fig. 3. Validation of selected AR targets antagonised by MYC overexpression. University of California, Santa Cruz (UCSC) genome browser visualisation of AR, MYC, H3K4me1, H3K4me3, H3K27ac, H3K27me3 and IgG binding events around the two well-established AR-target genes (a) KLK3 and (b) CAMKK2, which were antagonised by MYC overexpression. The binding events considered significant (p < 0.0001) and present in at least two biological replicates are indicated by the black boxes below the bigwig tracks provided. ChIP-qPCR validation of (c) AR and (d) MYC binding to enhancer regions of KLK3, CAMKK2, SOCS2, ERRFI1 and GNMT in LNCaP-MYC cells. (e–f) LNCaP-MYC cells were hormone-starved for 72 h and subsequently treated with 1 nM R1881, R1881 plus doxycycline (R1881 + Dox) or vehicle control for the indicated time points. (e) qRT-PCR validation of R1881-induction and repression through MYC overexpression of GNMT, SOCS2, ERRFI1, CAMKK2, and KLK3 transcripts in LNCaP-MYC cells (n = 3). (f) qRT-PCR for GNMT, SOCS2, ERRFI1, CAMKK2, and KLK3 transcripts upon knockdown of MYC in LNCaP and VCaP (n = 3). (g) Representative Western blot validation of R1881-induction and repression by MYC overexpression for CAMKK2, GNMT, and KLK3 at the indicated time points. Protein levels were normalized to GAPDH.

low staining for KLK3 and vice versa) (Fig. S9e–f). Taken together, these results imply that for certain markers an antagonistic relationship may exist and this merits further evaluation in larger cohorts.

4. Discussion

In this study we investigated the relationship between the AR and MYC, two crucial oncogenic transcription factors in PCa. MYC is known for supporting cell-specific gene programs and it is largely considered to be an amplifier of transcriptional activity (Nie et al., 2012).

However, a repressive function of MYC has previously been reported in lymphoma cells (van Riggelen et al., 2010). MYC amplification and overexpression are common in both breast and prostate cancer (Gurel et al., 2008; Jenkins et al., 1997; Singhi et al., 2012). In the apocrine breast cancer subtype MYC was found to enhance androgen responsive genes transcription (Ni et al., 2013). In contrast to this observation, we have identified an antagonistic relationship between the AR and MYC in PCa. This relationship is reflected at the gene expression level. In PCa, the concept of antagonism or reciprocity between other signaling networks and the AR has previously been described for ETS fusion
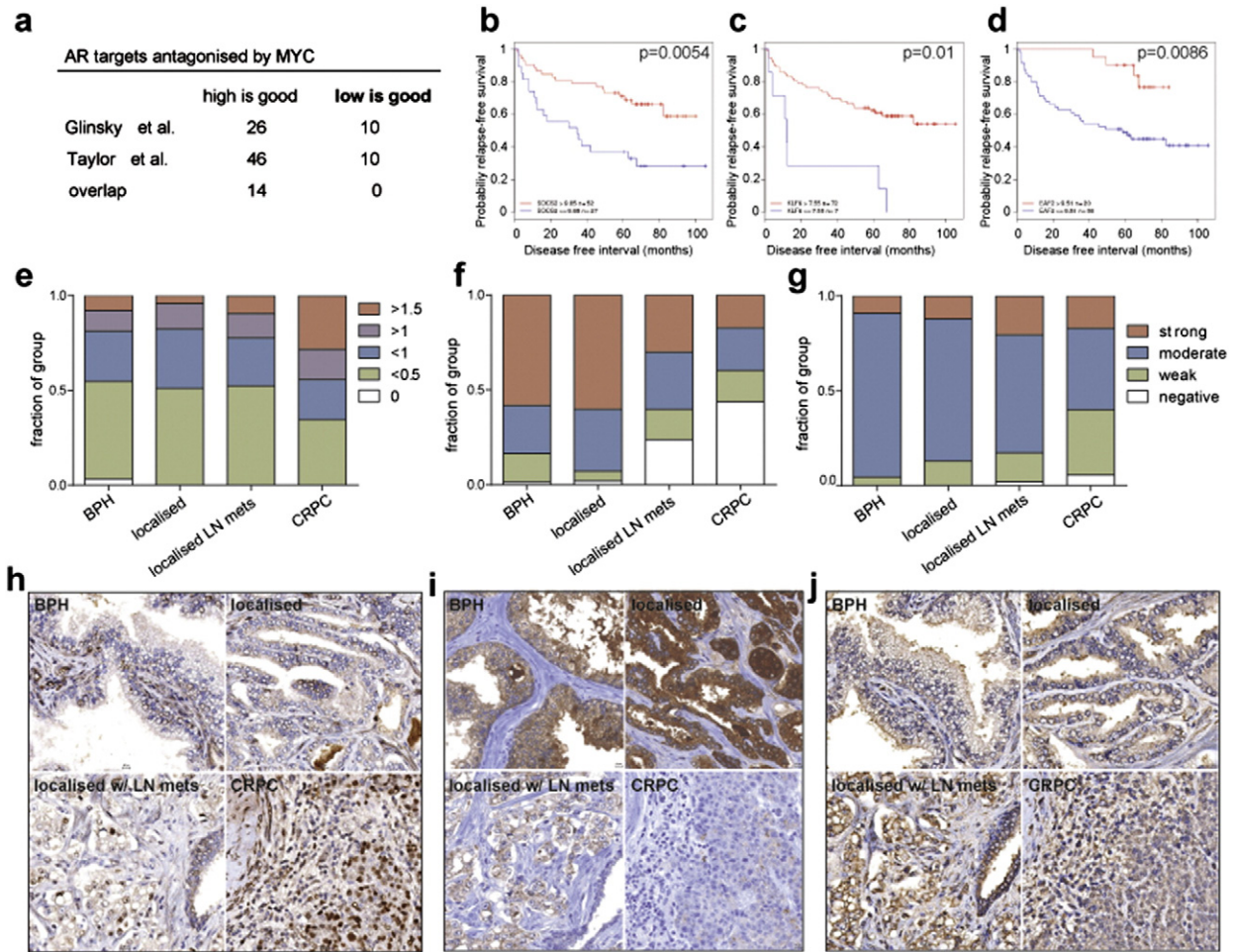
Fig. 4. MYC is inversely correlated with KLK3 and GNMT in prostate cancer patients with advanced disease. (a) Prognostic properties of R1881-induced genes antagonised by MYC overexpression in two publicly available clinical datasets (Glinsky et al., 2004; Taylor et al., 2010) and Kaplan-Meier survival curves for (b) SOCS2 (c) KLF6, and (d) EAF2. Proportions of specimens according to immunohistochemical staining intensities of (e) MYC, (f) KLK3 and (g) GNMT in patient samples of BPH (n = 68), localized PCa (n = 101), PCa with lymph node metastases (n = 71) and CRPC (n = 112). Nuclear staining for MYC was defined as percentage of stained nuclei multiplied by staining intensity. Staining intensities for KLK3 and GNMT were divided into four groups (negative, weak, moderate and strong). See supplemental information for details. Representative nuclear staining for (h) MYC, (i) cytoplasmic KLK3, and (j) GNMT in the indicated sample groups.

genes and the PI3-kinase (PI3K) pathway (Carver et al., 2011; Yu et al., 2010), and there is now good evidence that AR activation can repress PI3K/AKT signaling and vice versa (Carver et al., 2011; Wang et al., 2011b).

We profiled AR and MYC binding to chromatin and found that they co-occupy circa one third of the binding sites. We performed RIME and immunoprecipitation experiments in order to comment on how MYC antagonises AR activity but we did not find evidences of direct interaction between the two transcription factors. This suggests a more complex mechanism for the transcriptional interplay between AR and MYC. For instance, in the study by Ni and colleagues in breast cancer cells they show that the activation of the HER2/HER3 and PI3K/AKT signaling cascade by androgens/AR signaling results in decreased total MAD1 protein levels (Ni et al., 2013). MAD1 competes with MYC for the dimerization with MAX (Ayer et al., n.d.), and therefore MAD1 degradation leads to MYC activity. Thus, inhibition of AR by bicalutamide in breast cancer cells inhibits both AR and MYC activities (Ni et al., 2013). In prostate cancer patients, bicalutamide use is the standard of care but resistances to bicalutamide treatment emerge, and unlike for breast cancer (Mehta et al., 2015), expression of MAD1 is highly abundant and associated with disease progression (Varambally et al., 2005). Moreover, PI3K/AKT/mTOR signaling inhibits AR signaling via feedback inhibition of HER2/HER3 kinases. Viceversa, AR therapeutic inhibition activates AKT signaling by reducing levels of the AKT phosphatase

PHLPP (Carver et al., 2011). Therefore it is plausible to conclude that overexpressing MYC, a subset of tumours in castrate regimen could overcome MAD1 competition and be able to suppress a subset of AR target genes with such mechanism.

Interestingly, within the binding sites shared by AR and MYC, the most enriched motif was the one for binding of FOXA1. Further studies are needed to understand whether FOXA1 is involved in the interplay between AR and MYC. However, this conclusion would be in agreement with the study by Ni and colleagues by which MYC activation is context-specific thanks to the ability of co-opting the functions of other key transcription factors (Ni et al., 2013).

Performing RIME experiments, we also found components of the DNA replication and repairing machine as common interacting proteins between AR and MYC, which suggested that such interactions might indeed occur in condition of stress such as in MYC-overexpression induced DNA damage, as it was previously shown in other cell contexts (Vafa et al., 2002).

We also show that MYC overexpression is able to confer growth advantage only when cells are growing in castrate condition (in the absence of androgens), which is the condition mimicking most of the tumours in patients treated with the standard of care (castration/androgen deprivation therapy). A straightforward interpretation of these data is that the overexpression of MYC in cells exposed to castrate levels of androgens regulates the expression of a subset of genes in order to

overcome such stress. Conversely, when cells are exposed to androgens, the activated AR/androgen signaling pathway masks the effect of MYC activity. AR is then the main driver of cell growth. Therefore, the biological consequence of the transcriptional attenuation conferred by MYC overexpression may be a mechanistic insight into the ability of subtypes of PCa tumours to overcome stressful conditions such as DNA damage, and grow when patients are treated with AR-targeting therapies.

Our gene-level analysis of the interplay between AR and c-Myc shows that the transcriptional reprogramming of AR signaling by Myc has a reciprocal regulatory effect on genes regulating the epigenome and cell signaling including endogenous negative regulators of STAT signaling (SOCS2) and growth factor receptor signaling (ERRFI1), therefore extending the number of signaling pathways within such interplay.

Whilst this manuscript was in revision, Das and colleagues reported the selective advantage in promoting PCa metastasis upon inhibition of SOCS2 (Das et al., 2017), which is one of the genes we found to be attenuated by MYC overexpression. Furthermore, a re-analysis of a comprehensive study by Taylor and colleagues (Taylor et al., 2010) profiling transcriptomics of PCa showed that the expression of SOCS2 is lowest in metastases found in patients treated with castration (Fig. S10a). Again, another study by Iglesias-Gato et al. showed that high levels of SOCS2 protein are found in hormone naïve tumours compared to benign tissues, which is in agreement with the androgen regulation of such gene, but castration-resistant bone metastases show lower levels of SOCS2 than bone metastases in untreated patients (Iglesias-Gato et al., 2014).

Similarly, also GNMT displays lower transcripts levels in CRPCs than non-castrated metastatic PCa according to Taylor et al. (Taylor et al., 2010) (Fig. S10b), which suggests a similar involvement in attenuating metastatic potential.

Several of the antagonistically related genes from our study have previously been proposed as PCa biomarkers and appear to be negatively associated with MYC staining. Thus, future studies should focus on contextualising gene expression based on the expression and/or activity of oncogenic networks and transcription factors including and beyond the AR.

Supplementary data to this article can be found online at http://dx.doi.org/10.1016/j.ebiom.2017.04.006.

Funding Sources

Conflicts of Interest

The authors declare no competing interests.

Author Contributions

SJB designed and performed the experiments in the study, wrote the manuscript and analyzed the data. AU performed the bioinformatics analysis of the chromatin immunoprecipitation/sequencing data and wrote the manuscript. HMI and BT assisted in the preparation of the revised manuscript. LF undertook the immunohistochemistry and scoring of tissue microarrays and contributed to the drafting of the manuscript. PSR contributed to writing of the manuscript. SY contributed to the drafting of the manuscript. AMD evaluated tissue markers and undertook the pathology evaluation. IGM designed the study and wrote the manuscript.

Acknowledgements

References

Alvarez, S., Diaz, M., Flach, J., Rodriguez-Acebes, S., Lopez-Contreras, A.J., Martinez, D., Canamero, M., Fernandez-Capetillo, O., Isern, J., Passegue, E., et al., 2015. Replication stress caused by low MCM expression limits fetal erythropoiesis and hematopoietic stem cell functionality. Nat. Commun. 6, 8548.

Asangani, I.A., Dommeti, V.L., Wang, X., Malik, R., Cieslik, M., Yang, R., Escara-Wilke, J., Wilder-Romans, K., Dhanireddy, S., Engelke, C., et al., 2014. Therapeutic targeting of BET bromodomain proteins in castration-resistant prostate cancer. Nature 510, 278–282.

Ayer D.E., Kretzner L, Eisenman R.N. Mad: a heterodimeric partner for Max that antagonizes Myc transcriptional activity. Cell 72, 211–222.

Baena, E., Shao, Z., Linn, D.E., Glass, K., Hamblen, M.J., Fujiwara, Y., Kim, J., Nguyen, M., Zhang, X., Godinho, F.J., et al., 2013. ETV1 directs androgen metabolism and confers aggressive prostate cancer in targeted mice and patients. Genes Dev. 27, 683–698.

Barfeld, S.J., East, P., Zuber, V., Mills, I.G., 2014a. Meta-analysis of prostate cancer gene expression data identifies a novel discriminatory signature enriched for glycosylating enzymes. BMC Med. Genet. 7, 513.

Barfeld, S.J., Itkonen, H.M., Urbanucci, A., Mills, I.G., 2014b. Androgen-regulated metabolism and biosynthesis in prostate cancer. Endocr. Relat. Cancer 21, T57–T66.

Barfeld, S.J., Fazli, L., Persson, M., Marjavaara, L., Urbanucci, A., Kaukoniemi, K.M., Rennie, P.S., Ceder, Y., Chabes, A., Visakorpi, T., et al., 2015. Myc-dependent purine biosynthesis affects nucleolar stress and therapy response in prostate cancer. Oncotarget 6, 12587–12602.

Bernard, D., Pourtier-Manzanedo, A., Gil, J., Beach, D.H., 2003. Myc confers androgen-independent prostate cancer cell growth. J. Clin. Invest. 112, 1724–1731.

Carmona-Saez, P., Chagoyen, M., Tirado, F., Carazo, J.M., Pascual-Montano, A., 2007. GENECODIS: a web-based tool for finding significant concurrent annotations in gene lists. Genome Biol. 8, R3.

Carver, B.S., Chapinski, C., Wongvipat, J., Hieronymus, H., Chen, Y., Chandarlapaty, S., Arora, V.K., Le, C., Koutcher, J., Scher, H., et al., 2011. Reciprocal feedback regulation of PI3K and androgen receptor signaling in PTEN-deficient prostate cancer. Cancer Cell 19, 575–586.

Consortium, E.P, 2004. The ENCODE (ENCyclopedia Of DNA Elements) project. Science 306, 636–640.

Das, R., Gregory, P.A., Fernandes, R.C., Denis, I., Wang, Q., Townley, S.L., Zhao, S.G., Hanson, A.R., Pickering, M.A., Armstrong, H.K., et al., 2017. MicroRNA-194 promotes prostate cancer metastasis by inhibiting SOCS2. Cancer Res. 77, 1021–1034.

Dolganov, G.M., Maser, R.S., Novikov, A., Tosto, L., Chong, S., Bressan, D.A., Petrini, J.H., 1996. Human Rad50 is physically associated with human Mre11: identification of a conserved multiprotein complex implicated in recombinational DNA repair. Mol. Cell. Biol. 16, 4832–4841.

Ernst, J., Kheradpour, P., Mikkelsen, T.S., Shoresh, N., Ward, L.D., Epstein, C.B., Zhang, X., Wang, L., Issner, R., Coyne, M., et al., 2011. Mapping and analysis of chromatin state dynamics in nine human cell types. Nature 473, 43–49.

Gao, L., Schwartzman, J., Gibbs, A., Lisac, R., Kleinschmidt, R., Wilmot, B., Bottomly, D., Coleman, I., Nelson, P., McWeeney, S., et al., 2013. Androgen receptor promotes ligand-independent prostate cancer progression through c-Myc upregulation. PLoS One 8, e63563.

Gibson, S.I., Surosky, R.T., Tye, B.K., 1990. The phenotype of the minichromosome maintenance mutant mcm3 is characteristic of mutants defective in DNA replication. Mol. Cell. Biol. 10, 5707–5720.

Glinsky, G.V., Glinskii, A.B., Stephenson, A.J., Hoffman, R.M., Gerald, W.L., 2004. Gene expression profiling predicts clinical outcome of prostate cancer. J. Clin. Invest. 113, 913–923.

Gurel, B., Iwata, T., Koh, C.M., Jenkins, R.B., Lan, F., Van Dang, C., Hicks, J.L., Morgan, J., Cornish, T.C., Sutcliffe, S., et al., 2008. Nuclear MYC protein overexpression is an early alteration in human prostate carcinogenesis. Mod. Pathol. 21, 1156–1167.

Han, Z.D., Zhang, Y.Q., He, H.C., Dai, Q.S., Qin, G.Q., Chen, J.H., Cai, C., Fu, X., Bi, X.C., Zhu, J.G., et al., 2012. Identification of novel serological tumor markers for human prostate cancer using integrative transcriptome and proteome analysis. Med. Oncol. 29, 2877–2888.

Hoefer, J., Kern, J., Ofer, P., Eder, I.E., Schäfer, G., Dietrich, D., Kristiansen, G., Geley, S., Rainer, J., Gunsilius, E., et al., 2014. SOCS2 correlates with malignancy and exerts growth-promoting effects in prostate cancer. Endocr. Relat. Cancer 21, 175–187.

Hu, R., Lu, C., Mostaghel, E.A., Yegnasubramanian, S., Gurel, M., Tannahill, C., Edwards, J., Isaacs, W.B., Nelson, P.S., Bluemn, E., et al., 2012. Distinct transcriptional programs mediated by the ligand-dependent full-length androgen receptor and its splice variants in castration-resistant prostate cancer. Cancer Res. 72, 3457–3462.

Huang, Y.-C., Lee, C.-M., Chen, M., Chung, M.-Y., Chang, Y.-H., Huang, W.J.-S., Ho, D.M.-T., Pan, C.-C., Wu, T.T., Yang, S., et al., 2007. Haplotypes, loss of heterozygosity, and expression levels of glycine N-methyltransferase in prostate cancer. Clin. Cancer Res. 13, 1412–1420.

Hurtado, A., Holmes, K.A., Ross-Innes, C.S., Schmidt, D., Carroll, J.S., 2011. FOXA1 is a critical determinant of estrogen receptor function and endocrine response. Nat. Genet. 43, 27–33.

Iglesias-Gato, D., Chuan, Y.C., Wikstrom, P., Augsten, S., Jiang, N., Niu, Y., Seipel, A., Danneman, D., Vermeij, M., Fernandez-Perez, L., et al., 2014. SOCS2 mediates the cross talk between androgen and growth hormone signaling in prostate cancer. Carcinogenesis 35, 24–33.

Itkonen, H.M., Mills, I.G., 2013. N-linked glycosylation supports cross-talk between receptor tyrosine kinases and androgen receptor. PLoS One 8, e65016.

Itkonen, H.M., Minner, S., Guldvik, I.J., Sandmann, M.J., Tsourlakis, M.C., Berge, V., Svindland, A., Schlomm, T., Mills, I.G., 2013. O-GlcNAc transferase integrates metabolic pathways to regulate the stability of c-MYC in human prostate cancer cells. Cancer Res. 73, 5277–5287.

Jenkins, R.B., Qian, J., Lieber, M.M., Bostwick, D.G., 1997. Detection of c-myc oncogene amplification and chromosomal anomalies in metastatic prostatic carcinoma by fluorescence in situ hybridization. Cancer Res. 57, 524–531.

Jentzmik, F., Stephan, C., Miller, K., Schrader, M., Erbersdobler, A., Kristiansen, G., Lein, M., Jung, K., 2010. Sarcosine in urine after digital rectal examination fails as a marker in prostate cancer detection and identification of aggressive tumours. Eur. Urol. 58, 12–18 (discussion 20-11).

Jozwik, K.M., Chernukhin, I., Serandour, A.A., Nagarajan, S., Carroll, J.S., 2016. FOXA1 directs H3K4 Monomethylation at enhancers via recruitment of the methyltransferase MLL3. Cell Rep. 17, 2715–2723.

Jung, C., Kim, R.S., Zhang, H.J., Lee, S.J., Jeng, M.H., 2004. HOXB13 induces growth suppression of prostate cancer cells as a repressor of hormone-activated androgen receptor signaling. Cancer Res. 64, 9185–9192.

Kato, G.J., Lee, W.M., Chen, L.L., Dang, C.V., 1992. Max: functional domains and interaction with c-Myc. Genes Dev. 6, 81–92.

Khan, A.P., Rajendiran, T.M., Ateeq, B., Asangani, I.A., Athanikar, J.N., Yocum, A.K., Mehra, R., Siddiqui, J., Palapattu, G., Wei, J.T., et al., 2013. The role of sarcosine metabolism in prostate cancer progression. Neoplasia 15, 491–501.

Kim, S.D., Park, R.Y., Kim, Y.R., Kim, I.J., Kang, T.W., Nam, K.I., Ahn, K.Y., Bae, C.S., Kim, B.Y., Park, S.S., et al., 2010. HOXB13 is co-localized with androgen receptor to suppress androgen-stimulated prostate-specific antigen expression. Anat. Cell Biol. 43, 284–293.

Koh, C.M., Gurel, B., Sutcliffe, S., Aryee, M.J., Schultz, D., Iwata, T., Uemura, M., Zeller, K.I., Anele, U., Zheng, Q., et al., 2011a. Alterations in nucleolar structure and gene expression programs in prostatic neoplasia are driven by the MYC oncogene. Am. J. Pathol. 178, 1824–1834.

Koh, C.M., Iwata, T., Zheng, Q., Bethel, C., Yegnasubramanian, S., De Marzo, A.M., 2011b. Myc enforces overexpression of EZH2 in early prostatic neoplasia via transcriptional and post-transcriptional mechanisms. Oncotarget 2, 669–683.

Kokontis, J., Takakura, K., Hay, N., Liao, S., 1994. Increased androgen receptor activity and altered c-myc expression in prostate cancer cells after long-term androgen deprivation. Cancer Res. 54, 1566–1573.

Lee, D.K., Park, J.H., Kim, J.H., Lee, S.J., Jo, M.K., Gil, M.C., Song, K.H., Park, J.W., 2010. Progression of prostate cancer despite an extremely low serum level of prostate-specific antigen. Korean J. Urol. 51, 358–361.

Lima, A.R., Bastos Mde, L., Carvalho, M., Guedes de Pinho, P., 2016. Biomarker discovery in human prostate cancer: an update in metabolomics studies. Transl. Oncol. 9, 357–370.

Liu, X., Gomez-Pinillos, A., Loder, C., Carrillo-de Santa Pau, E., Qiao, R., Unger, P.D., Kurek, R., Oddoux, C., Melamed, J., Gallagher, R.E., et al., 2012. KLF6 loss of function in human prostate cancer progression is implicated in resistance to androgen deprivation. Am. J. Pathol. 181, 1007–1016.

Lupien, M., Eeckhoute, J., Meyer, C.A., Wang, Q., Zhang, Y., Li, W., Carroll, J.S., Liu, X.S., Brown, M., 2008. FoxA1 translates epigenetic signatures into enhancer driven lineage-specific transcription. Cell 132, 958–970.

Madine, M.A., Khoo, C.Y., Mills, A.D., Laskey, R.A., 1995. MCM3 complex required for cell cycle regulation of DNA replication in vertebrate cells. Nature 375, 421–424.

Massie, C.E., Lynch, A., Ramos-Montoya, A., Boren, J., Stark, R., Fazli, L., Warren, A., Scott, H., Madhu, B., Sharma, N., et al., 2011. The androgen receptor fuels prostate cancer by regulating central metabolism and biosynthesis. EMBO J. 30, 2719–2733.

McMahon, S.B., Van Buskirk, H.A., Dugan, K.A., Copeland, T.D., Cole, M.D., 1998. The novel ATM-related protein TRRAP is an essential cofactor for the c-Myc and E2F oncoproteins. Cell 94, 363–374.

Mehta, J., Asthana, S., Mandal, C.C., Saxena, S., 2015. A molecular analysis provides novel insights into androgen receptor signalling in breast cancer. PLoS One 10, e0120622.

Mohammed, H., D'Santos, C., Serandour, A.A., Ali, H.R., Brown, G.D., Atkins, A., Rueda, O.M., Holmes, K.A., Theodorou, V., Robinson, J.L., et al., 2013. Endogenous purification reveals GREB1 as a key estrogen receptor regulatory factor. Cell Rep. 3, 342–349.

Mohammed, H., Taylor, C., Brown, G.D., Papachristou, E.K., Carroll, J.S., D'Santos, C.S., 2016. Rapid immunoprecipitation mass spectrometry of endogenous proteins (RIME) for analysis of chromatin complexes. Nat. Protoc. 11, 316–326.

Nelson, P.S., Clegg, N., Arnold, H., Ferguson, C., Bonham, M., White, J., Hood, L., Lin, B., 2002. The program of androgen-responsive genes in neoplastic prostate epithelium. Proc. Natl. Acad. Sci. U. S. A. 99, 11890–11895.

Ni, M., Chen, Y., Fei, T., Li, D., Lim, E., Liu, X.S., Brown, M., 2013. Amplitude modulation of androgen signaling by c-MYC. Genes Dev. 27, 734–748.

Nie, Z., Hu, G., Wei, G., Cui, K., Yamane, A., Resch, W., Wang, R., Green, D.R., Tessarollo, L., Casellas, R., et al., 2012. C-Myc is a universal amplifier of expressed genes in lymphocytes and embryonic stem cells. Cell 151, 68–79.

Paull, T.T., Rogakou, E.P., Yamazaki, V., Kirchgessner, C.U., Gellert, M., Bonner, W.M., 2000. A critical role for histone H2AX in recruitment of repair factors to nuclear foci after DNA damage. Curr. Biol. 10, 886–895.

Pellakuru, L.G., Iwata, T., Gurel, B., Schultz, D., Hicks, J., Bethel, C., Yegnasubramanian, S., De Marzo, A.M., 2012. Global levels of H3K27me3 track with differentiation in vivo and are deregulated by MYC in prostate cancer. Am. J. Pathol. 181, 560–569.

Rahl, P.B., Lin, C.Y., Seila, A.C., Flynn, R.A., McCuine, S., Burge, C.B., Sharp, P.A., Young, R.A., 2010. c-Myc regulates transcriptional pause release. Cell 141, 432–445.

Ramos-Montoya, A., Lamb, A.D., Russell, R., Carroll, T., Jurmeister, S., Galeano-Dalmau, N., Massie, C.E., Boren, J., Bon, H., Theodorou, V., et al., 2014. HES6 drives a critical AR transcriptional programme to induce castration-resistant prostate cancer through activation of an E2F1-mediated cell cycle network. EMBO Mol. Med. 6, 651–661.

van Riggelen, J., Müller, J., Otto, T., Beuger, V., Yetil, A., Choi, P.S., Kosan, C., Möröy, T., Felsher, D.W., Eilers, M., 2010. The interaction between Myc and Miz1 is required to antagonize TGFbeta-dependent autocrine signaling during lymphoma formation and maintenance. Genes Dev. 24, 1281–1294.

Robinson, D., Van Allen, E.M., Wu, Y.-M., Schultz, N., Lonigro, R.J., Mosquera, J.-M., Montgomery, B., Taplin, M.-E., Pritchard, C.C., Attard, G., et al., 2015. Integrative clinical genomics of advanced prostate cancer. Cell 161, 1215–1228.

Sahu, B., Laakso, M., Ovaska, K., Mirtti, T., Lundin, J., Rannikko, A., Sankila, A., Turunen, J.-P., Lundin, M., Konsti, J., et al., 2011. Dual role of FoxA1 in androgen receptor binding to chromatin, androgen signalling and prostate cancer. EMBO J. 30, 3962–3976.

Schuhmacher, M., Kohlhuber, F., Holzel, M., Kaiser, C., Burtscher, H., Jarsch, M., Bornkamm, G.W., Laux, G., Polack, A., Weidle, U.H., et al., 2001. The transcriptional program of a human B cell line in response to Myc. Nucleic Acids Res. 29, 397–406.

Sella, A., Konichezky, M., Flex, D., Sulkes, A., Baniel, J., 2000. Low PSA metastatic androgen-independent prostate cancer. Eur. Urol. 38, 250–254.

Serandour, A.A., Brown, G.D., Cohen, J.D., Carroll, J.S., 2013. Development of an Illumina-based ChIP-exonuclease method provides insight into FoxA1-DNA binding properties. Genome Biol. 14, R147.

Singhi, A.D., Cimino-Mathews, A., Jenkins, R.B., Lan, F., Fink, S.R., Nassar, H., Vang, R., Fetting, J., Hicks, J., Sukumar, S., et al., 2012. MYC Gene amplification is often acquired in lethal distant breast cancer metastases of unamplified primary tumors. Mod. Pathol. 25, 378–387.

Sreekumar, A., Poisson, L.M., Rajendiran, T.M., Khan, A.P., Cao, Q., Yu, J., Laxman, B., Mehra, R., Lonigro, R.J., Li, Y., et al., 2009. Metabolomic profiles delineate potential role for sarcosine in prostate cancer progression. Nature 457, 910–914.

Taylor, B.S., Schultz, N., Hieronymus, H., Gopalan, A., Xiao, Y., Carver, B.S., Arora, V.K., Kaushik, P., Cerami, E., Reva, B., et al., 2010. Integrative genomic profiling of human prostate cancer. Cancer Cell 18, 11–22.

Urbanucci, A., Sahu, B., Seppala, J., Larjo, A., Latonen, L.M., Waltering, K.K., Tammela, T.L., Vessella, R.L., Lahdesmaki, H., Janne, O.A., et al., 2012. Overexpression of androgen receptor enhances the binding of the receptor to the chromatin in prostate cancer. Oncogene 31, 2153–2163.

Vafa, O., Wade, M., Kern, S., Beeche, M., Pandita, T.K., Hampton, G.M., Wahl, G.M., 2002. c-Myc can induce DNA damage, increase reactive oxygen species, and mitigate p53 function: a mechanism for oncogene-induced genetic instability. Mol. Cell 9, 1031–1044.

Varambally, S., Dhanasekaran, S.M., Zhou, M., Barrette, T.R., Kumar-Sinha, C., Sanda, M.G., Ghosh, D., Pienta, K.J., Sewalt, R.G., Otte, A.P., et al., 2002. The polycomb group protein EZH2 is involved in progression of prostate cancer. Nature 419, 624–629.

Varambally, S., Yu, J., Laxman, B., Rhodes, D.R., Mehra, R., Tomlins, S.A., Shah, R.B., Chandran, U., Monzon, F.A., Becich, M.J., et al., 2005. Integrative genomic and proteomic analysis of prostate cancer reveals signatures of metastatic progression. Cancer Cell 8, 393–406.

Waltering, K.K., Helenius, M.A., Sahu, B., Manni, V., Linja, M.J., Janne, O.A., Visakorpi, T., 2009. Increased expression of androgen receptor sensitizes prostate cancer cells to low levels of androgens. Cancer Res. 69, 8141–8149.

Waltering, K.K., Urbanucci, A., Visakorpi, T., 2012. Androgen receptor (AR) aberrations in castration-resistant prostate cancer. Mol. Cell. Endocrinol. 360, 38–43.

Wang, Q., Li, W., Liu, X.S., Carroll, J.S., Janne, O.A., Keeton, E.K., Chinnaiyan, A.M., Pienta, K.J., Brown, M., 2007. A hierarchical network of transcription factors governs androgen receptor-dependent prostate cancer growth. Mol. Cell 27, 380–392.

Wang, D., Garcia-Bassets, I., Benner, C., Li, W., Su, X., Zhou, Y., Qiu, J., Liu, W., Kaikkonen, M.U., Ohgi, K.A., et al., 2011a. Reprogramming transcription by distinct classes of enhancers functionally defined by eRNA. Nature 474, 390–394.

Wang, Y., Romigh, T., He, X., Tan, M.H., Orloff, M.S., Silverman, R.H., Heston, W.D., Eng, C., 2011b. Differential regulation of PTEN expression by androgen receptor in prostate and breast cancers. Oncogene 30, 4327–4338.

Xiao, W., Zhang, Q., Jiang, F., Pins, M., Kozlowski, J.M., Wang, Z., 2003. Suppression of prostate tumor growth by U19, a novel testosterone-regulated apoptosis inducer. Cancer Res. 63, 4698–4704.

Yu, J., Yu, J., Mani, R.-S., Cao, Q., Brenner, C.J., Cao, X., Wang, X., Wu, L., Li, J., Hu, M., et al., 2010. An integrated network of androgen receptor, polycomb, and TMPRSS2-ERG gene fusions in prostate cancer progression. Cancer Cell 17, 443–454.

Zhang, Y., Liu, T., Meyer, C.A., Eeckhoute, J., Johnson, D.S., Bernstein, B.E., Nusbaum, C., Myers, R.M., Brown, M., Li, W., et al., 2008. Model-based analysis of ChIP-Seq (MACS). Genome Biol. 9, R137.

Zhu, J.-G., Dai, Q.-S., Han, Z.-D., He, H.-C., Mo, R.-J., Chen, G., Chen, Y.-F., Wu, Y.-D., Yang, S.-B., Jiang, F.-N., et al., 2013. Expression of SOCSs in human prostate cancer and their association in prognosis. Mol. Cell. Biochem. 381, 51–59.